



OPEN

Cross-talk between dopamine and noradrenaline modulates glutamatergic transmission in the deep cerebellar nuclei

Fumihito Saitow[✉], Ryosuke Arakawa & Hidenori Suzuki

Modulation of synaptic transmission in the deep cerebellar nuclei, a major output region of the cerebellum, is essential for regulating motor and non-motor functions by controlling information flow from the cerebellar cortex. In this study, we aimed to investigate the effects of dopamine (DA) and noradrenaline (NA) on glutamatergic synaptic transmission using cerebellar slices from both male and female Wistar rats. Stimulation-evoked excitatory postsynaptic currents (eEPSCs) were recorded from deep cerebellar nuclei neurons using whole-cell patch-clamp technique. Bath application of DA or NA decreased the eEPSC amplitude. Pharmacological analysis revealed presynaptic D2-like receptors (D2R) and α_2 -adrenergic receptors (α_2 -AdR) as mediators of the inhibitory effects induced by DA and NA, respectively. While DA decreased eEPSC amplitude in all tested synapses, the selective D2R agonist, quinpirole showed no effect in approximately 30% of synapses. By contrast, NA and α_2 -AdR-selective agonists (clonidine and dexmedetomidine) inhibited synaptic transmission in all tested synapses. Notably, both DA and NA maintained their inhibitory effects even when their respective receptor antagonists (sulpiride and RS79948), were present. This observation suggests cross-receptor interactions: DA acted through α_2 -AdRs, while NA operated via D2Rs. These findings reveal novel cross-talk of catecholamines within cerebellar networks, providing new insights into mechanisms underlying synaptic modulation.

Keywords Deep cerebellar nuclei, Glutamatergic synaptic transmission, α_2 -adrenergic receptor, D₂ dopaminergic receptor, Modulation, Cross-talk

The mammalian cerebellum receives catecholaminergic input that is widely recognized as noradrenergic rather than dopaminergic. This projection to the cerebellum is speculated to consist of noradrenergic fibers originating from the locus coeruleus due to the low levels of dopamine (DA) detected in this brain region¹. Consequently, the cerebellum has not been traditionally included in DA-regulated neural circuitry. However, several anatomical studies have suggested the existence of sparse but distinct dopaminergic projections from midbrain structures, including the ventral tegmental area and substantia nigra, to the cerebellum²⁻⁵. Moreover, Purkinje cells in certain regions of the cerebellar cortex may contribute to dopamine release into the DCN^{6,7}. These findings have led to a growing interest in the potential role of DA in cerebellar function, although its extent and functional relevance remain debated. While the cerebellum expresses fewer DA receptors compared with other brain regions⁸, studies have reported DA binding⁵, DA transporters, neuronal tyrosine hydroxylase expression^{3,9}, and DA receptors^{10,11} within the cerebellum. These findings suggest that DA plays important roles as a neurotransmitter or neuromodulator in the cerebellum. DA receptors are generally classified into two families: the G_s-coupled D1-like receptors (D₁ and D₅) and the G_{i/o}-coupled D2-like receptors (D₂, D₃, and D₄)¹². The expression of these receptors in the cerebellum⁸ implicates them in various physiological functions and the pathogenesis of psychiatric disorders¹³⁻¹⁶. Despite these associations, few electrophysiological studies have demonstrated DAergic responses in the cerebellum¹⁷⁻¹⁹. By contrast, noradrenaline (NA), another catecholamine, is well known to modulate both GABAergic²⁰⁻²⁴ and glutamatergic^{18,25,26} synaptic transmission in the cerebellum.

NAergic neurons from the locus coeruleus project afferent fibers to both the cerebellar cortex²⁷ and deep cerebellar nuclei (DCN)^{28,29}. The DCN are the main output centers of the cerebellum, projecting to premotor centers in the forebrain, inferior olive in the brainstem, and thalamus³⁰. Recent studies have demonstrated that

Department of Pharmacology, Nippon Medical School, Tokyo 113-8602, Japan. [✉]email: f-saitow@nms.ac.jp

glutamatergic neurons in the DCN form monosynaptic connections with the ventral tegmental area (VTA)³¹ and substantia nigra³², both of which are dopaminergic centers. The VTA and substantia nigra, in turn, project to the frontal cortex and striatum, respectively, regions critical for controlling reward, motivation, cognition, and vigor. These findings indicate that the activity of DCN neurons may play a crucial role in higher cognitive functions in addition to motor control. Given the increasing number of studies associating the cerebellum with cognitive functions^{2,31–33}, understanding the modulatory effects of DA on cerebellar output is vital. Although dopaminergic systems influence cerebellar cortical outputs, the direct effects of DA on glutamatergic synaptic transmission within the DCN, a key node in cerebellar output, remain largely unknown.

The present study investigates the modulatory effects of DA and NA on glutamatergic synapses within the DCN. Through electrophysiological recordings, the research aims to determine how these catecholamines influence excitatory synaptic transmission, thereby elucidating their distinct and potentially complementary roles in cerebellar function. Elucidating the complex interplay of neurotransmitters within cerebellar circuitry will provide new insights into the mechanisms underlying synaptic modulation. Further, understanding the regulatory mechanisms of synaptic transmission has important implications for both normal and pathological cerebellar function. These findings will enhance our understanding of cerebellar neurotransmission and advance knowledge of motor and cognitive processes regulated by cerebellar circuits.

Results

DA decreased the amplitude of glutamatergic excitatory postsynaptic currents in DCN neurons

In the presence of gabazine and strychnine, which block GABAergic and glycinergic transmission, electrical stimulation via glass microelectrodes placed in the white matter elicited eEPSCs in DCN neurons at a membrane potential (V_h) of -70 mV. Bath application of DA at a concentration of 10 μM significantly decreased the eEPSC amplitude to $49.1 \pm 3.9\%$ of baseline levels before DA application in all tested DCN neurons (Fig. 1A). This inhibitory effect on eEPSC amplitude was completely reversed within 20 min after washing out the DA-containing ACSF (Fig. 1A). To determine whether DA exerts its inhibitory effects at presynaptic or postsynaptic sites, we measured changes in the PPR before and during DA application. In the control medium, paired-pulse stimulation with an inter-stimulus interval of 50 ms produced EPSCs with a mean PPR of 0.71 ± 0.04 . As shown in Fig. 1B, DA significantly increased the PPR to 0.88 ± 0.06 during DA application ($t(10) = -4.81$, $p = 7.1 \times 10^{-4}$, paired t -test, $n = 11$). Furthermore, eEPSCs were measured to estimate the fractional change of coefficient of variation (CV^{-2})³⁴. As shown in Fig. 1C, most of the data points were distributed in the section below the identity line (dotted line); that is, the magnitude of decrease in the ratio of CV^{-2} (baseline/DA treatment) was greater than that in the mean eEPSC amplitude, and this difference was statistically significant ($t(10) = -5.21$, $p = 4.0 \times 10^{-4}$, paired t -test, $n = 11$). These results suggest that DA-induced depression of eEPSC amplitudes may be attributable to presynaptic inhibition of glutamate release. The effect of DA (1 – 20 μM) on eEPSC amplitude depression was concentration-dependent (Fig. 1D). The best fitting of the concentration–response curve revealed an IC_{50} of 1.86 μM , an extent of depression (y_{\max}) of 49.26% of the baseline, and a Hill coefficient (n) of 1.57 (Fig. 1D).

NA decreased the amplitude of glutamatergic excitatory postsynaptic currents in DCN neurons via α_2 -adrenaline receptor activation

Bath application of 10 μM NA significantly decreased the eEPSC amplitude in all tested DCN neurons (Fig. 2A). The maximum extent of depression induced by 10 μM NA, observed 4 – 5 min after application, reached $42.5 \pm 6.2\%$ of the baseline eEPSC amplitude ($n = 5$). The inhibitory effect of NA on eEPSCs was more pronounced than that of DA, but the difference was not statistically significant ($t(14) = -1.30$, $p = 0.26$, unpaired t -test). Similar to the inhibitory action of DA, an increase in the PPR following NA administration (Fig. 2B, control: 0.72 ± 0.06 ; NA application: 0.86 ± 0.07 ; $t(4) = -3.46$, $p = 0.026$, paired t -test, $n = 5$) and the results of CV^{-2} analysis (Fig. 2C) strongly suggested that the eEPSC amplitude suppressed by NA is also mediated by a presynaptic mechanism. The concentration–response curve showed a maximum inhibition (y_{\max}) of 64.9 , an IC_{50} value of 0.59 μM , and a Hill coefficient (n) of 0.86 (Fig. 2D).

To determine the AdR subtypes responsible for the depression of eEPSC amplitudes in DCN neurons, we examined the effects of the α_1 -AdR agonist phenylephrine (PE) and the α_2 -AdR agonist clonidine (Clon). PE induced a slight decrease in the eEPSC amplitude ($89.8 \pm 1.1\%$ of the baseline) without changing PPR (Fig. 2E; control: 0.71 ± 0.03 ; PE application: 0.72 ± 0.03 ; $t(6) = -0.63$, $p = 0.55$, paired t -test, $n = 7$). By contrast, Clon administration irreversibly decreased eEPSC amplitude ($70.9 \pm 3.5\%$ of the baseline, $n = 7$) while increasing PPR (control: 0.73 ± 0.03 ; Clon: 0.86 ± 0.02 ; $t(6) = -7.14$, $p = 3.8 \times 10^{-4}$, paired t -test, $n = 7$). Similarly, the selective α_2 -AdR agonist dexmedetomidine (Dex) exhibited a time course of inhibitory action comparable to that of clonidine ($59.6 \pm 6.7\%$ of the baseline) and significantly increased PPR (Fig. 2F; control: 0.77 ± 0.04 ; Dex: 0.97 ± 0.06 ; $t(8) = -4.09$, $p = 3.4 \times 10^{-4}$, paired t -test, $n = 9$). These findings indicate that NA suppresses excitatory synaptic transmission in DCN neurons predominantly via presynaptic α_2 -adR activation.

D2-like receptor agonist did not affect some synapses in DCN

The inhibitory effect of DA on synaptic transmission is generally attributed to the activation of G_i -coupled D2-like receptors (D2Rs). To investigate this mechanism, we pharmacologically assessed the effects of the D2R agonist, quinpirole (QPR). Pooled data from all experiments showed that 5 μM QPR clearly decreased the eEPSC amplitude ($78.7 \pm 5.6\%$ of the baseline, $n = 14$). However, $6/14$ synapses examined were insensitive to QPR and showed no notable reduction in eEPSC amplitudes following QPR application ($93.9 \pm 6.0\%$ of the baseline, $n = 6$, “Non-responder” in the inset of Fig. 3A). For further analysis, synapses in which drug application suppressed synaptic currents to 90% or less of the baseline were classified as ‘Responders,’ whereas those maintaining more than 90% of the baseline amplitude were classified as ‘Non-Responders.’ In some cases, as

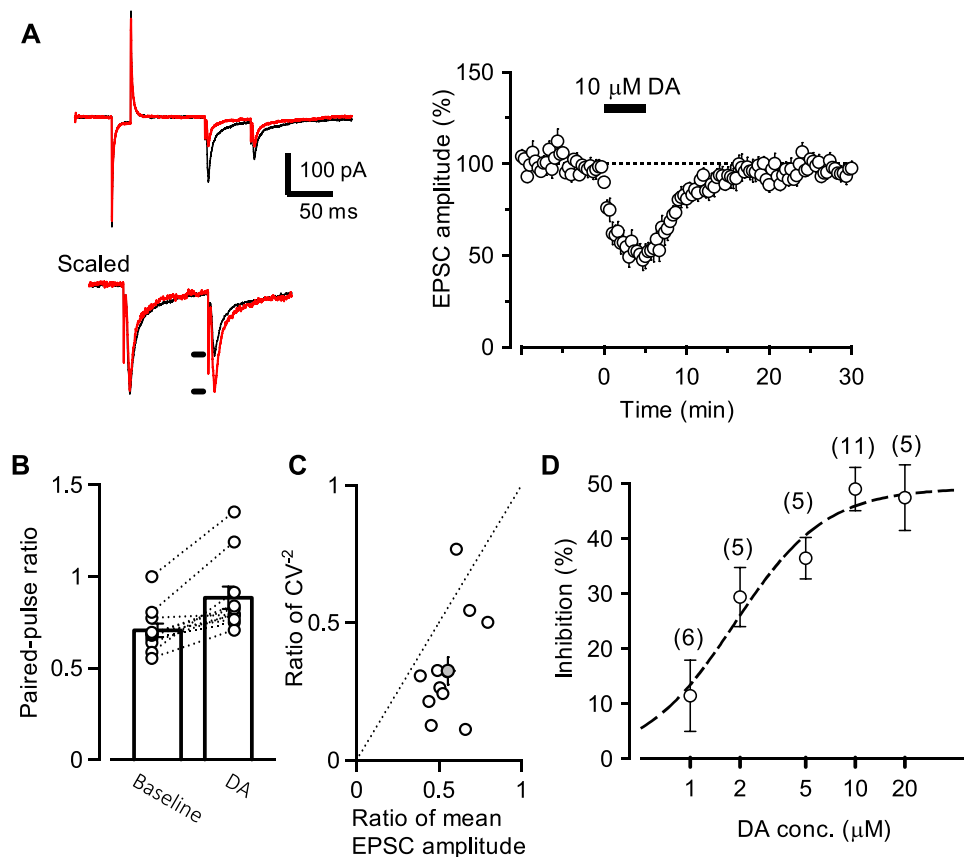


Fig. 1. Dopamine (DA) decreased evoked excitatory postsynaptic current (eEPSC) amplitude. **A:** Inhibitory effect of DA on eEPSC amplitude. Left: Application of 10 μ M DA markedly decreased the eEPSC amplitude (red traces). The averaged traces (black trace: baseline for 2 min; red trace: after 5–7 min DA application) were scaled to the amplitude of the first EPSC and superimposed for comparison. This result suggests that the DA-induced inhibitory effect involves a presynaptic mechanism. Right: Time course of changes in eEPSC amplitude induced by 10 μ M DA in deep cerebellar nuclei neurons. **B:** Increase in paired-pulse ratio (PPR) during DA application. A paired-pulse protocol with a 50-ms interval was applied. PPRs were recorded before (baseline) and 5–7 min after 10- μ M DA application (DA). A significant increase in PPR was observed after DA application. Each column represents the mean \pm SEM. **C:** Variance analysis of eEPSC in DCN neurons. The ratio of CV^{-2} was plotted against the ratio of the mean eEPSC amplitude ($n=11$). Both CV^{-2} and the mean eEPSC amplitude were determined by using 10 sweeps before and during the application of 10 μ M DA. The filled circle represents means \pm SEM. **D:** Concentration–response curve for DA-induced inhibition. The extent of eEPSC inhibition at different DA concentrations was plotted, representing the effects observed 5–7 min after DA application. Data are the least-mean square fit to a concentration–response curve with the Hill coefficient. Each point represents the mean \pm SEM. The numbers adjacent to each point indicate the number of experiments.

shown in Fig. 3B, “Responder” synapses exhibited an irreversible and substantial inhibition of eEPSC amplitude (“Responder”: $67.2 \pm 6.0\%$ of the baseline, $n=8$). Additionally, even “Non-responder” synapses to QPR exhibited distinct inhibitory effects when exposed to DA, as shown in Fig. 3C. These results suggest two key points: (1) Glutamatergic synaptic terminals in the DCN exhibit heterogeneity in D2R expression. (2) DA may activate receptors other than D2Rs to exert inhibitory effects.

DA-induced inhibitory action was partially sustained under D2R blocking condition

As previously mentioned, DA may presynaptically act on receptors other than D2Rs at glutamatergic synaptic terminals. Therefore, we investigated the role of α_2 -AdR activation in the inhibitory effects of DA and NA under conditions of D2R blockade. To test the hypothesis that α_2 -AdR activation contributes to the inhibitory effects of DA, experiments were conducted using the D₂- and D₃-receptor antagonist sulpiride to block D2Rs. In the presence of 2 μ M sulpiride, the inhibitory effects of QPR were completely blocked ($98.1 \pm 0.5\%$ of the baseline, $n=9$, Fig. 4A). Conversely, Clon (5 μ M) still significantly inhibited the amplitude of eEPSC across all tested synapses ($73.4 \pm 2.4\%$ of the baseline, $n=8$, Fig. 4A). The extent of eEPSC suppression caused by Clon was comparable ($t(13) = -0.56$, $p=0.59$, unpaired t -test) to that shown in Fig. 2E ($70.9 \pm 3.5\%$, $n=7$). After confirmation of sulpiride’s blocking efficacy, DA and NA were sequentially applied with intervals of more than 30 min under D2R blockade. As shown in Fig. 4B, DA slightly inhibited eEPSC amplitude ($84.7 \pm 3.8\%$ of the

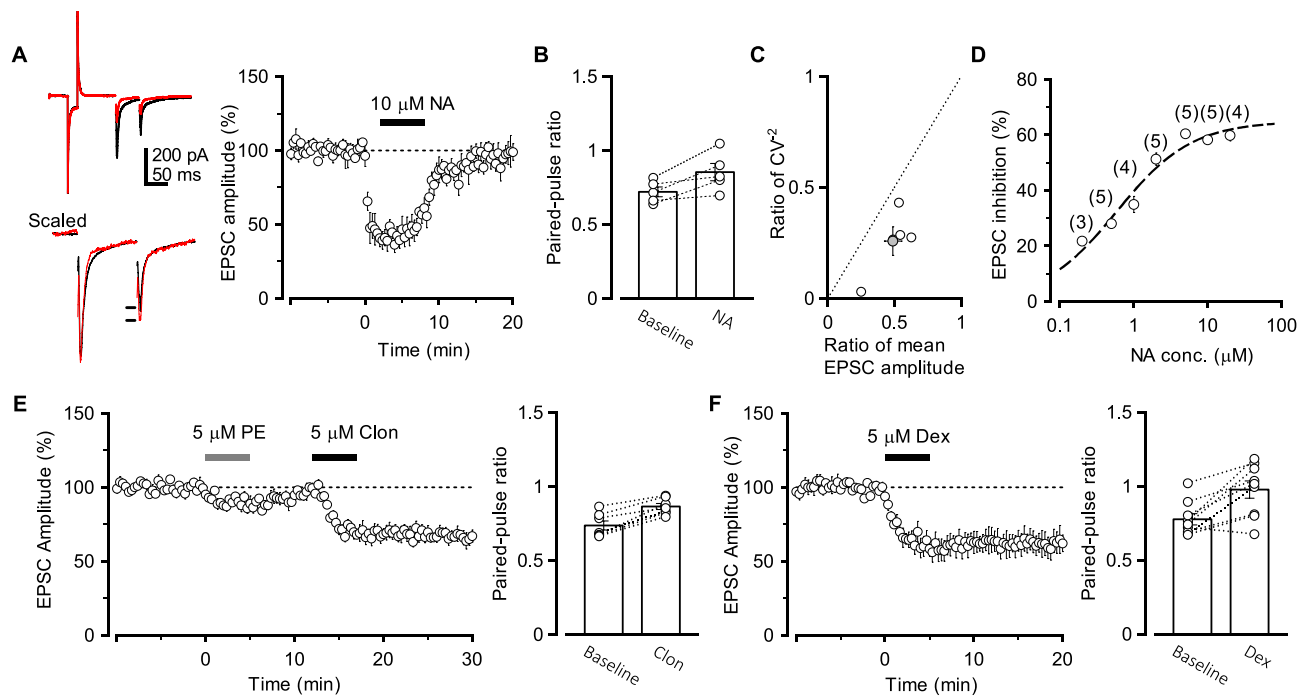


Fig. 2. Noradrenaline (NA) decreased the amplitude of eEPSCs via α_2 -AdR activation. **A:** Inhibitory effect of NA on eEPSC amplitude. Left: Application of 10 μ M NA markedly decreased the eEPSC amplitude (red trace). The traces shown are the averages of eight consecutive responses (black trace: baseline for 2 min; red trace: after 5–7 min of NA application). Right: Time course of changes in eEPSC amplitude induced by 10 μ M NA in deep cerebellar nuclei neurons. **B:** Increase in PPR during NA application. PPRs were recorded before (Baseline) and 5–7 min after 10- μ M NA application (NA). A significant increase in PPR was observed after NA application. Each column represents the mean \pm SEM. **C:** Variance analysis of eEPSC in DCN neurons before and during the NA application. The ratio of CV^{-2} was plotted against the ratio of the mean eEPSC amplitude ($n=5$). Both CV^{-2} and the mean eEPSC amplitude were determined by using 10 sweeps before and during the application of 10 μ M NA. The filled circle represents means \pm SEM. **D:** Concentration–response curves illustrating NA’s effects. Each data point represents the extent of eEPSC inhibition following a 5-min NA application at the corresponding concentration. Data are the least-mean square fit to a concentration–response curve with the Hill coefficient. Each point represents the mean \pm SEM. The numbers adjacent to each point indicate the number of experiments. **E** and **F:** Pharmacological experiments revealed that the NA-induced inhibitory effect was mediated by α_2 -adrenergic receptor (α_2 -AdR) activation. The α_2 -AdR agonists clonidine (E) and dexmedetomidine (F) significantly decreased EPSC amplitude (left panels) and increased paired-pulse ratio (right panels) in deep cerebellar nuclei neurons. Conversely, the α_1 -adrenergic receptor agonist phenylephrine caused a slight decrease in eEPSC amplitude. However, PE application did not alter the paired-pulse ratio, suggesting that the underlying mechanism differs from the inhibitory effects associated with α_2 -AdR activation.

baseline, $n=7$, Fig. 4B) despite the presence of sulpiride, although the suppression was significantly weaker compared with experiments without the D2R antagonist ($t(13)=-4.24$, $p=9.4 \times 10^{-4}$; vs. 53.3% of the baseline as shown in Fig. 1A and 1C). These findings indicate that D2R activation by DA is primarily responsible for EPSC amplitude suppression. However, substantial non-D2R contributions, presumably through α_2 -AdR activation, were also identified. Moreover, NA-induced inhibition of eEPSC amplitude was also affected under D2R blockade ($66.2 \pm 5.3\%$ of the baseline, $n=7$), with suppression levels significantly reduced compared with those observed without the antagonist ($t(10)=-2.88$, $p=0.016$; vs. 42.5% of the baseline shown in Fig. 2A and 2B). These results suggest that DA and NA interact with α_2 -AdRs and D2Rs in mediating their inhibitory effects.

DA-induced inhibitory action correlated with sensitivity to D2R agonist

Given the dual involvement of α_2 -AdRs and D2Rs in the actions of DA and NA, we examined the inhibitory effects of these neurotransmitters under conditions of α_2 -AdR blockade using the potent and selective antagonist RS79948³⁵. In the presence of 1 μ M RS79948, DA and QPR were sequentially administered with intervals exceeding 30 min. As previously described, synaptic responses to DA were also classified into two groups: “Responders” (filled circles in Fig. 5A) and “Non-responders” (open circles in Fig. 5A). Approximately 75% (14/19) of synapses exhibited less than 90% inhibition of eEPSC amplitude by DA and were categorized as “Responders” (filled circles in Fig. 5A; DA: $79.4 \pm 1.1\%$; QPR: $86.5 \pm 1.2\%$, $n=14$), while the remaining $\sim 25\%$ were less responsive to DA (open circles in Fig. 5A; DA: $95.0 \pm 0.9\%$; QPR: $93.0 \pm 1.2\%$, $n=5$). As shown in Fig. 5B, a strong correlation was observed between the extent of inhibition by DA and QPR ($r^2=0.71$). These

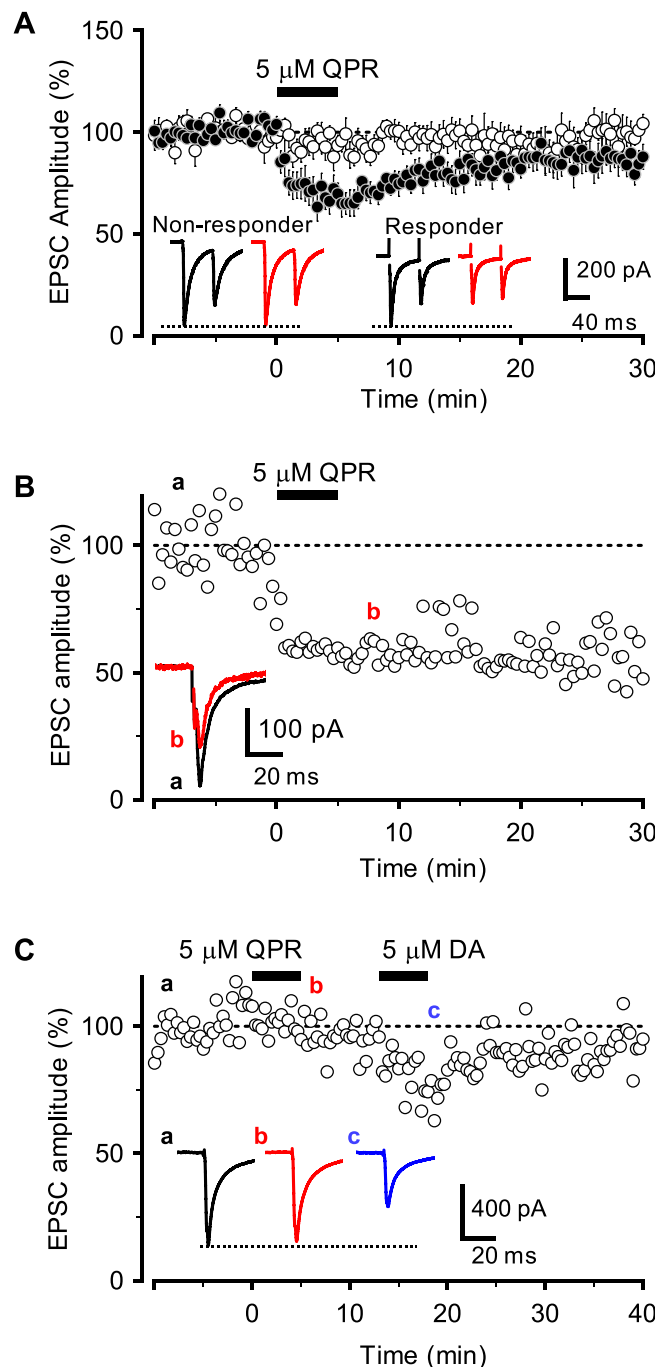


Fig. 3. Application of a D2-like receptor (D2R) agonist did not affect all synapses in the deep cerebellar nuclei. **A:** Effects of the D2R agonist, quinpirole (QPR) on glutamatergic synapses in deep cerebellar nuclei neurons. Application of QPR induced a significant inhibitory effect on eEPSC amplitude in a subset of synapses classified as “Responders” (filled circles; right inset traces; $n=8$). In contrast, no substantial inhibition was observed in the remaining synapses, termed “Non-responders,” which showed no more than 90% inhibition by QPR (open circles; left inset traces; $n=6$). **B:** Representative time course showing QPR-induced inhibition of eEPSC amplitude. Most synapses were inhibited by QPR application. The traces labeled **a** and **b** were obtained at the indicated time points in the graph and are superimposed for comparison (inset). **C:** Representative time course of a non-responder (QPR-insensitive) synapse. Approximately 30% of synapses did not show inhibitory effects following QPR application (traces **a** and **b** in the inset, before and after QPR application, respectively). By contrast, dopamine showed inhibitory effects (trace **c**, after DA application, in the inset). These results suggest that D2R-induced inhibitory effects exhibit heterogeneity due to variable receptor expression at glutamatergic synaptic terminals.

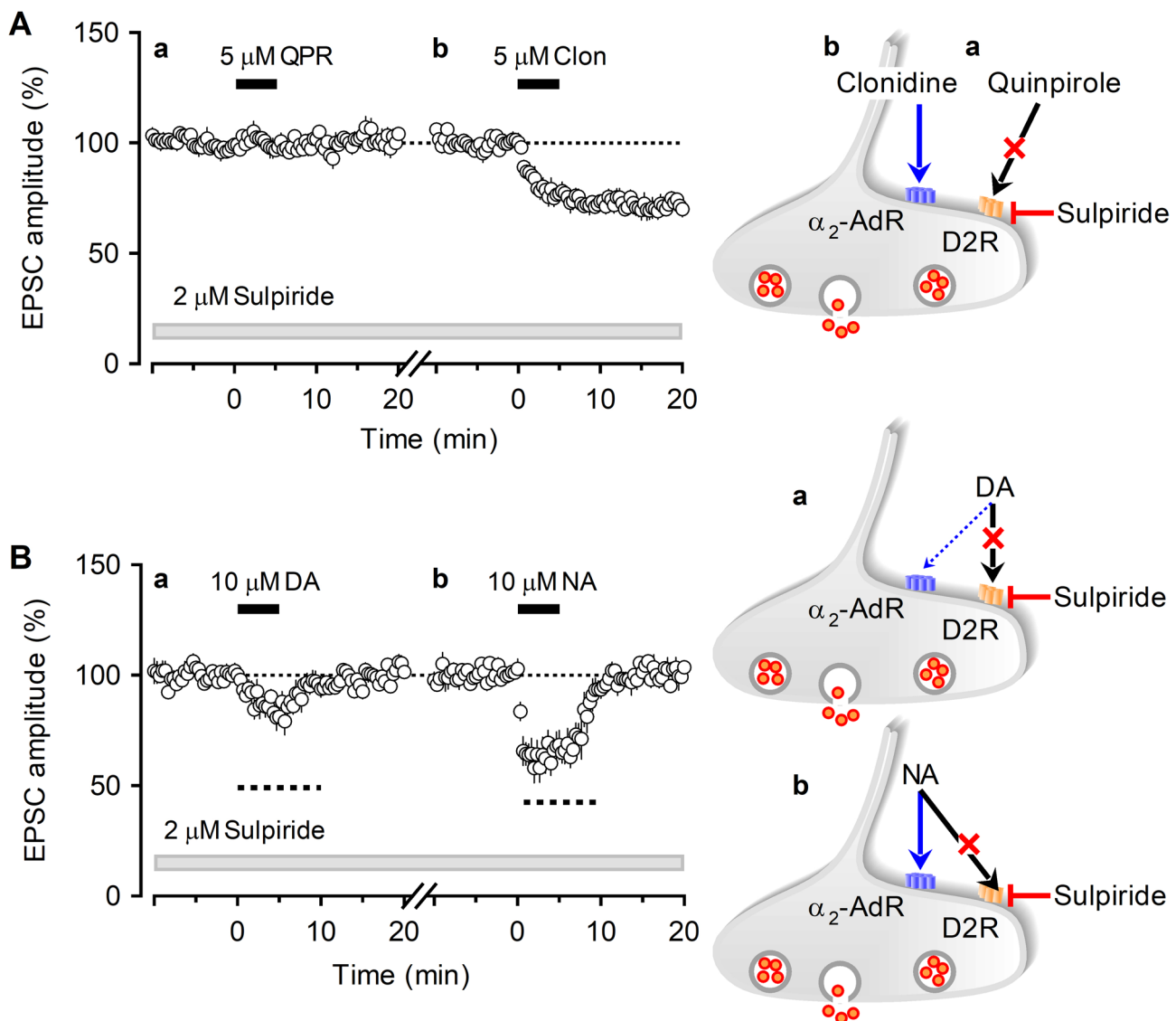


Fig. 4. Dopamine (DA)-induced inhibitory action correlated with sensitivity to the D2-like receptor (D2R) agonist. **A:** In the presence of the D2R antagonist sulpiride, the effect of QPR was completely blocked (**a**), whereas the inhibitory action induced by the α_2 -AdR agonist clonidine (Clon) remained unaffected (**b**). A schematic drawing of the action sites of the two types of catecholaminergic receptors is shown on the right. **B:** Despite the blocking of D2Rs by sulpiride, DA-induced suppression was partially sustained (**a**). Blocking D2Rs also affected NA-induced suppression of eEPSC amplitude. The dotted lines represent the extent of eEPSC amplitude suppression observed in the absence of receptor antagonists. These results suggest that DA and NA may activate α_2 -AdRs and D2Rs, respectively. A schematic drawing of the action sites of DA and NA is shown on the right.

results suggest that approximately 25% of glutamatergic synaptic terminals in the DCN express little to no D2Rs. This variation in D2R expression likely explains the heterogeneity in sensitivity to QPR in the results demonstrated in Fig. 3.

NA-induced inhibitory action was partially sustained under α_2 -AdR blocking condition

The results above suggest that both NA and DA mutually interact with α_2 -AdRs and D2Rs. Further analysis was conducted to examine whether NA could inhibit the eEPSC amplitude under the blockade of α_2 -AdRs. When 1 μ M RS79948 was applied, the NA-induced inhibitory action was apparently suppressed on average across all collected data (Fig. 6A, $97.0 \pm 1.1\%$, $n = 20$). However, some synapses still exhibited clear inhibitory effects, as shown in Fig. 6B (filled circles, $88.0 \pm 0.8\%$, $n = 5$). Conversely, 15 of 20 synapses showed no inhibitory action in response to NA application (open circles in Fig. 6B, $100.1 \pm 0.5\%$, $n = 15$). These observations imply that 75% of the synapses expressed only α_2 -AdRs, while the remaining 25% (5 of 20 synapses) exhibited inhibitory effects despite the blockade of α_2 -AdRs, suggesting that NA may have activated D2Rs. Subsequently, the effects of DA on the eEPSC amplitude were evaluated under the blockade of α_2 -AdRs. If all glutamatergic synaptic terminals

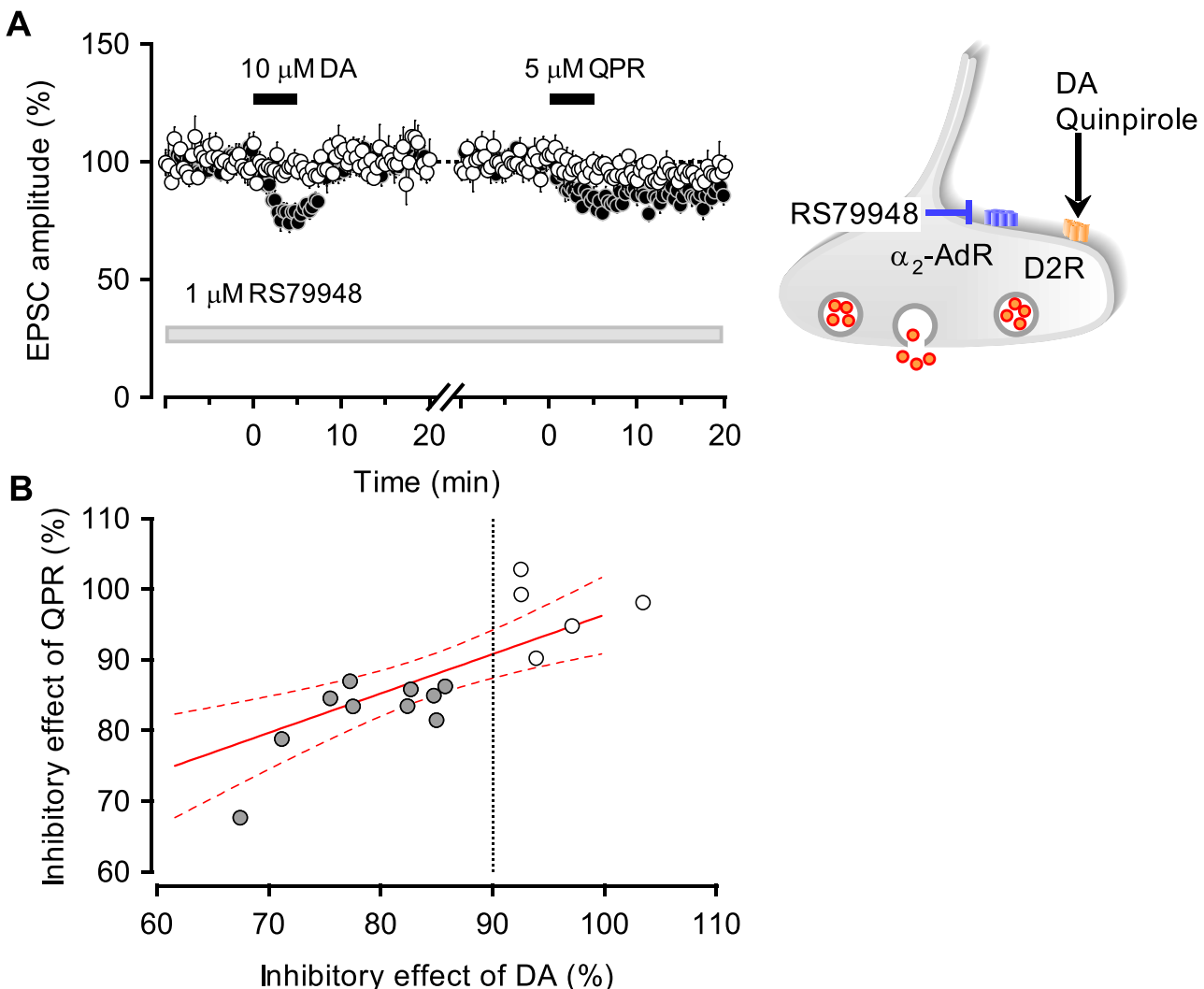


Fig. 5. Dopamine (DA)-induced inhibitory action correlated with sensitivity to the D2-like receptor (D2R) agonist. **A:** In the presence of the α_2 -AdR antagonist RS79948, the DA-induced inhibitory effect was reduced on average. Pooled data from 14 experiments revealed that DA application decreased eEPSC amplitude below 90% of the baseline in nine cases, which were selected and plotted (filled circles, $n=9$). Following DA application, the D2R agonist quinpirole (QPR) was applied. Five synapses tested showed reduced sensitivity to DA, with eEPSC amplitude remaining above 90% of the baseline (open circles, $n=5$). Modulatory effects of QPR were similarly less effective at these synapses. A schematic drawing of the action sites of the two types of catecholaminergic receptors is shown on the right. **B:** A highly significant correlation was observed between the inhibitory effects of QPR and DA-induced inhibition under conditions where α_2 -AdRs were blocked ($r^2=0.71$).

expressed D2Rs, the inhibitory effects of DA should have been observable in all tests. In the presence of 1 μ M RS79948, DA-induced inhibitory action was significantly observed on average (Fig. 7A, $87.3 \pm 0.7\%$, $n=21$). Within this dataset, under the blockade of α_2 -AdRs, the extent of synapses responsive to DA was $81.6 \pm 0.9\%$ ($n=12$; filled circles in Fig. 7B). The extent of inhibition by DA was noticeably reduced in this setting compared with conditions without D2R and α_2 -AdR antagonists (Fig. 1). Notably, approximately 40% of the synapses (nine of 21 synapses) showed little or no inhibitory effect on the eEPSC amplitude (open circles in Fig. 7B, $95.5 \pm 0.9\%$, $n=9$). This result aligned with that presented in Fig. 5, in which five of 19 synapses were categorized as "Non-responders." These results strongly suggest that DA can activate both D2Rs and α_2 -AdRs.

NA and DA did not produce inhibitory effects under both blocking conditions

Based on previous results, neither NA nor DA would produce inhibitory effects under conditions where both D2Rs and α_2 -AdRs were blocked. To confirm this, we conducted an experiment using an antagonist cocktail targeting both receptor types. Under these conditions, DA- and NA-induced inhibitory actions were completely blocked in all cases without exception (Fig. 8A, DA: $97.0 \pm 0.8\%$, $n=16$; NA: $100.5 \pm 1.4\%$, $n=16$). Taken together,

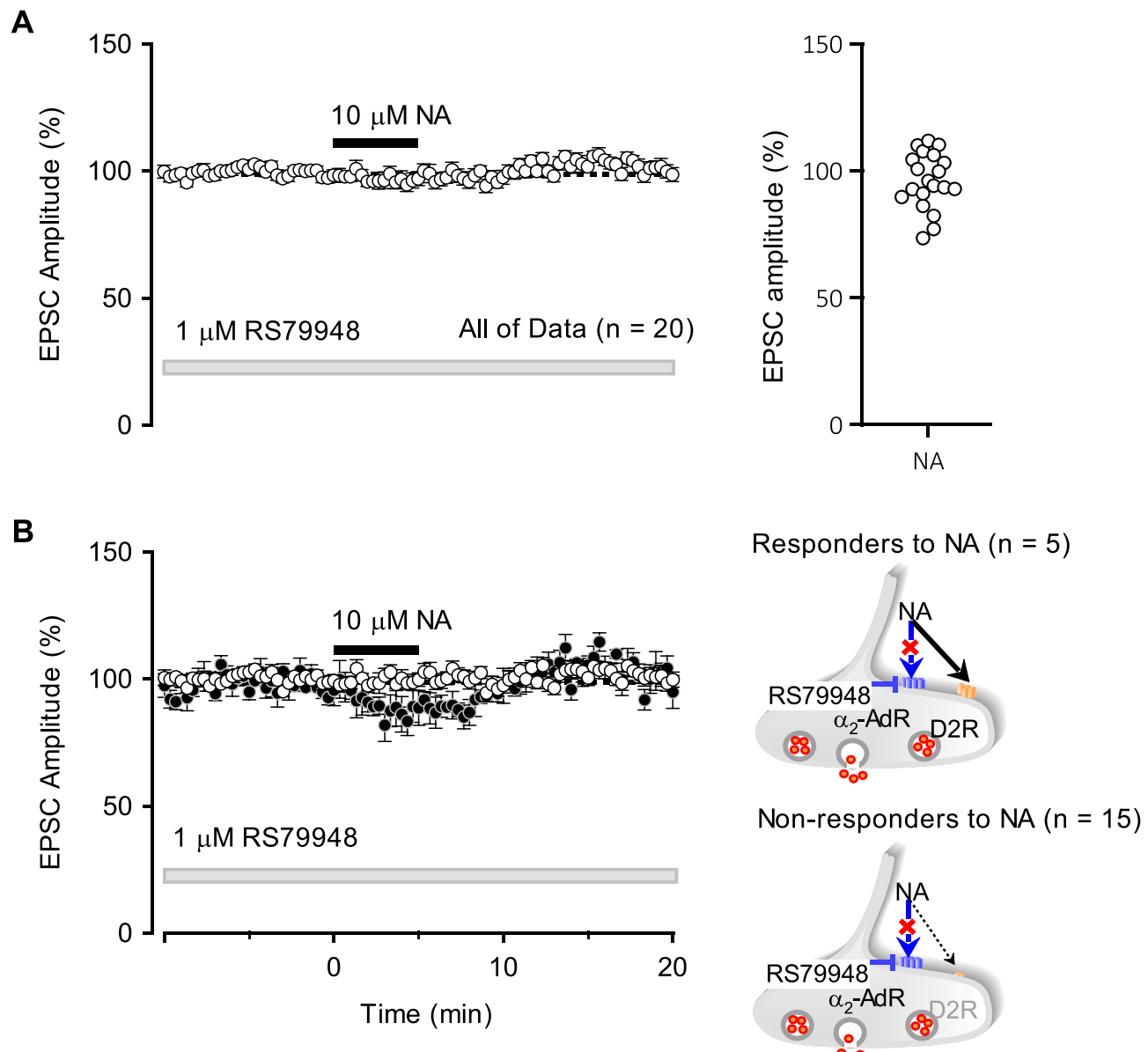


Fig. 6. Effects of α_2 -AdR antagonists on noradrenaline (NA)-induced inhibitory action. **A:** In the presence of the α_2 -AdR antagonist RS79948, the NA-induced inhibitory action was suppressed on average across all recorded data ($n=20$). Right: Distribution of eEPSC amplitudes after 5–7 min of NA application. **B:** Five out of 20 data were less affected by the α_2 -AdR antagonist and clearly showed inhibitory effects in deep cerebellar nuclei neurons (filled circles, $n=5$). This observation suggests that NA activated D2-like receptors (D2Rs) in these cases, as shown in the schematic drawing (right). In 15 out of 20 data, no effect of NA application was observed (open circles, $n=15$). These results suggest that a subset of synapses in the deep cerebellar nuclei heterogeneously express DA receptors. Schematic drawing on the right shows “Non-responder” synapses with no or extremely low D2-like receptor expression under α_2 -AdR blockade conditions.

these results indicate that the modulatory effects of DA and NA on glutamatergic synapses onto DCN neurons involve both D2Rs and α_2 -AdRs. Additionally, each transmitter interacts with the receptor system of the other.

Discussion

This study provides novel insights into the modulatory mechanisms of glutamatergic neurotransmission in DCN neurons, particularly highlighting the complex interplay between DAergic and NAergic actions. The findings demonstrate mutual cross-talk between these neurotransmitter systems, offering significant implications for understanding cerebellar function. To the best of our knowledge, this study is the first to demonstrate such cross-talk at DCN synapses.

The results show that DA and NA individually exert inhibitory effects on glutamatergic synapses in DCN neurons. Notably, the dopaminergic inhibitory action is mediated through presynaptic D2Rs, representing

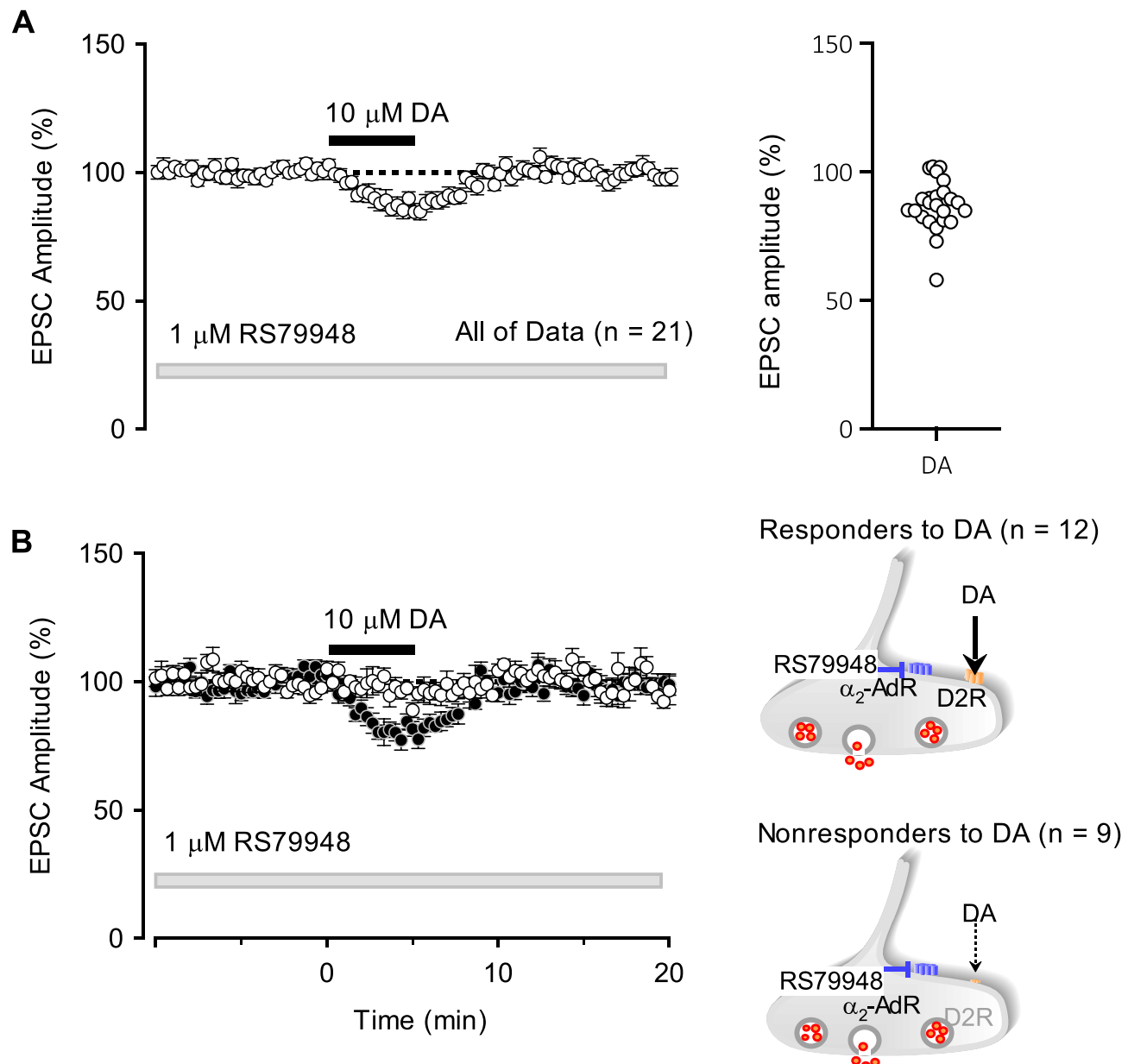


Fig. 7. Effects of α_2 -AdR antagonists on DA-induced inhibitory action. **A:** The α_2 -AdR antagonist RS79948 significantly reduced the DA-induced inhibitory action when analyzing all obtained data (n = 21). Right: Distribution of eEPSC amplitudes after 5–7 min of DA application. **B:** Twelve out of 21 data showed a clear inhibitory effect on deep cerebellar nuclei neurons (filled circles, n = 12). This suggests that DA acted on expressed DA receptors, as shown in the schematic drawing (right). In 9 out of 21 data, DA application had no observable effect (open circles, n = 9). These results suggest that D2-like receptors were heterogeneously expressed in certain synapses of the deep cerebellar nuclei, as shown in the schematic drawing under the condition of α_2 -AdR blockade.

a novel finding in synaptic modulation within the DCN. To our knowledge, there have been no previous immunohistochemical studies reporting D2Rs expression in the DCN. This contributes to our understanding of DA's role in the cerebellum, an area of increasing research interest^{2,33,36}. Moreover, the results suggest that DA's inhibitory effect is not exclusively dependent on D2Rs but also involves α_2 -AdRs. Similarly, NA's inhibitory effect is not solely mediated by α_2 -AdRs but also involves D2Rs. While previous studies have reported cross-talk in which DA activates α_2 -AdRs^{37–40} and NA activates D2Rs^{41–43} in other neurons, our findings demonstrate that both types of cross-talk occur at glutamatergic synaptic terminals in the DCN (Fig. 8B). The structural similarities between DA and NA may explain their ability to bind to both receptor types. Regarding NA-activated D2Rs, the D₄ receptor subtype, which has a relatively high affinity for NA, stands out (K_i (nM), DA: 2.2 \pm 0.16 vs. NA: 31 \pm 9.2⁴¹). Although D₄ receptors are associated with neuronal metabolic activity⁴⁴, they are expressed at very low levels in the cerebellum¹⁰. In this study, the effects of the D2R agonist QPR were completely blocked

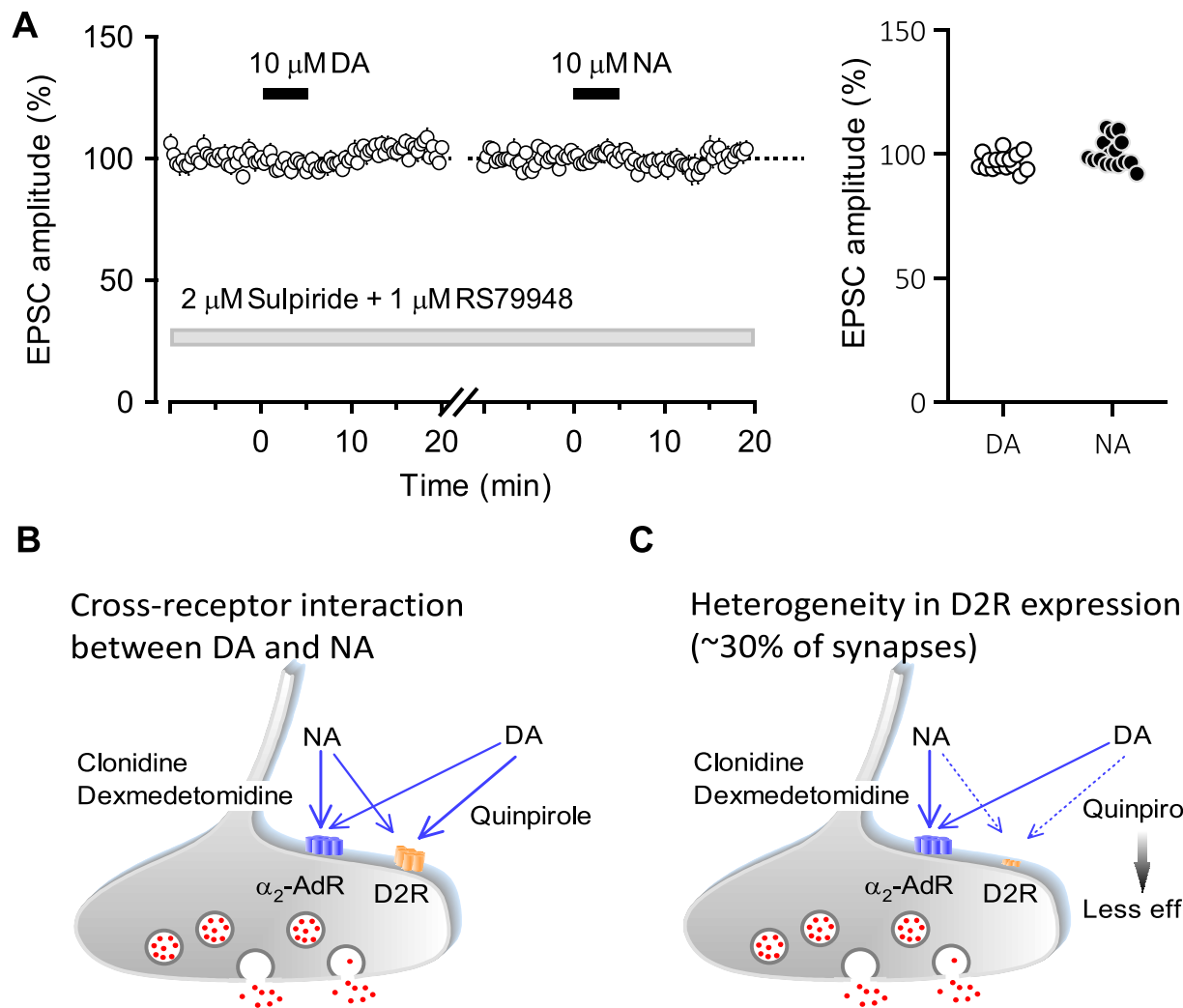


Fig. 8. A: Effects of α_2 -AdR and D2R antagonist cocktails on DA- and NA-induced inhibitory actions. The combined presence of RS79948 and sulpiride, α_2 -AdR and D2R antagonists, respectively, completely blocked the DA- and NA-induced inhibitory actions ($n=16$). Right panel shows the distributions of eEPSC amplitudes after 5–7 min of DA and NA application. B: Cross-receptor interactions and heterogeneity of receptor expression underlying catecholaminergic modulation of glutamatergic synaptic transmission in the DCN. Schematic illustration of cross-receptor interactions between DA and NA at the presynaptic terminal of glutamatergic synapses in the DCN. The results demonstrate that DA can act on α_2 -AdRs and NA on D2Rs, indicating cross-receptor interactions. C: Illustration of synapse-to-synapse heterogeneity in D2R expression. Pharmacological experiments using the D2R agonist, quinpirole and DA in the presence of α_2 -AdR blockade revealed that approximately 30% of synapses lack functional D2R expression. In contrast, applications of α_2 -AdR agonists and NA consistently showed inhibitory effect across all synapses.

by 2 μ M sulpiride. Given sulpiride's high affinity for D₂ and D₃ receptors, but low affinity for D₄ receptors, the results suggest that the D2Rs expressed at glutamatergic terminals in the DCN are likely D₂ or D₃ receptors.

The complementary nature of these modulatory actions suggests a sophisticated mechanism for fine-tuning glutamatergic synaptic transmission. At the neuronal circuit level, this heterogeneous dual-receptor system appears to regulate the dynamic range of inhibitory control over glutamatergic transmissions. This regulation allows for precise modulation of cerebellar output and synaptic plasticity. Such an arrangement enhances flexibility in synaptic regulation, enabling the circuit to adapt to varying physiological demands. For instance, our previous study reported that 5-HT, another modulatory amine, modulates the extent of long-term depression at mossy fiber synapses onto DCN neurons by reducing group I metabotropic glutamate receptor-mediated slow EPSCs⁴⁵. Furthermore, NA-induced α_2 -AdR activation has been shown to reduce associative plasticity by decreasing glutamate release at climbing fiber synapses, thereby decreasing climbing fiber-evoked dendritic calcium signals in the cerebellar cortex¹⁸. Although the synaptic terminals of the climbing fiber express D2Rs, the heterogeneity and cross-talk with α_2 -AdRs had not been reported prior to this study. Therefore, our findings on dual aminergic receptor interactions may represent a novel mechanism for fine-tuning neural transmission in the DCN. This

complex regulation could provide a cellular foundation for the precise control of motor coordination and non-motor functions¹⁶ associated with cerebellar circuits.

Quantitative analysis of synaptic inhibition provided insights into the relative contributions of these catecholaminergic receptor systems. The IC_{50} values for DA (1.86 μ M) and NA (0.59 μ M) suggest that α_2 -AdR-mediated effects predominate in terms of potency. This conclusion is supported by experiments using a selective D2R agonist and a potent α_2 -AdR antagonist (Figs. 3, 6, and 7), which demonstrate differential receptor expression patterns at synaptic terminals. Approximately 30% (25–40%) of synapses expressed D2Rs, whereas a larger proportion, remained 70%, expressed α_2 -AdRs (Fig. 8C). These results indicate that the heterogeneity of both D2R and α_2 -AdR expression at synaptic terminals is involved in synaptic regulation, with α_2 -AdRs playing a more significant role.

The source of catecholamines likely does not involve direct dopaminergic innervation from the VTA and substantia nigra^{2,4}, although the presence of local dopaminergic circuits and microdomains of DA transmission cannot be completely ruled out. Some cerebellar Purkinje cells expressing tyrosine hydroxylase in the posterior and lateral cerebellum may be involved in DA release into the DCN^{6,7}. However, the predominance of α_2 -AdR-mediated modulatory action suggests that NA serves as the primary neuromodulator. Moreover, DA is present as a precursor in NAergic nerve fibers, highlighting its close connection to neurotransmitter synthesis pathways. Serving as a critical intermediate in NA biosynthesis, DA undergoes conversion during the synthesis from tyrosine. The locus coeruleus (LC) emerges as the most plausible source of DA and NA. Projections from the LC to the DCN area¹⁶, along with its release of DA in various cortical regions⁴⁶, including the hippocampus⁴⁷ and thalamus⁴⁸, reinforce its role. This synthetic pathway and anatomical projection pattern further support the LC as a crucial source of both DA and NA neurotransmitters in the DCN.

This study demonstrated the presence of cross-talk between α_2 -AdR and D2Rs through the use of receptor-specific agonists and antagonists. Careful consideration must be given to the specificity of the pharmacological tools used. A recent study highlighted that RS79948, used as an α_2 -AdR antagonist, may also exhibit blocking effects on D2Rs⁴⁹. Despite concerns about potential interference with dopaminergic signaling by RS79948, both DA and QPR retained their ability to induce inhibitory actions in its presence (Fig. 5). Furthermore, a significant correlation between the inhibitory effects of DA and QPR suggested that D2R activation remained functionally intact under these conditions (Fig. 5). This observation provides substantial evidence that RS79948 did not significantly interfere with D2R function in the experimental setup. Another concern in the experimental design was the potential for receptor desensitization, particularly in experiments where DA and NA were applied consecutively (Figs. 3, 4, and 8). However, the results indicate that desensitization did not occur under the experimental conditions. Previous studies have demonstrated that catecholaminergic receptor responses recover to their initial magnitude after a 20-min interval following a 5-min NA or DA application⁵⁰. In this study, a minimum interval of 30 min was allowed between catecholamine administrations, ensuring sufficient time for receptor reactivity to recover fully. These findings suggest that the observed cross-talk effects were receptor-mediated responses rather than artifacts of receptor desensitization. An additional concern was the use of relatively young rats (postnatal days 11–15) in these experiments, necessitated by technical limitations in obtaining electrophysiological recordings from mature animals. The expression ratios and functional roles of catecholaminergic receptors, as well as tyrosine-related pathways, are likely to undergo developmental changes as the cerebellum matures. Future studies using immunohistochemical and biochemical approaches will be required to investigate receptor expression patterns in adult rats and to trace developmental changes in these systems.

These findings contribute valuable insights into the role of aminergic modulation in cerebellar function and dysfunction. Future studies should investigate the physiological significance of this cross-talk in motor or non-motor functions, as well as its potential implications for neurological disorders affecting cerebellar function.

Methods

Slice preparation

Experiments were performed using thin slices of the cerebellum from Wistar rats (postnatal days 11–15)^{45,51,52}. Both male and female animals were deeply anesthetized through isoflurane inhalation (approximately 3% in air, v/v), and their brains were rapidly removed. The cerebella were then dissected out from the extracted brains and parasagittal cerebellar slices of 250- μ m thickness were sectioned using a vibratome (VT1000S or VT1200S; Leica, Germany) at 4 °C in cutting solution that contained the following compounds: 299.2 mM sucrose, 3.4 mM KCl, 0.3 mM CaCl₂, 3.0 mM MgCl₂, 10 mM HEPES, 0.6 mM NaH₂PO₄, and 10 mM glucose. The slices were then placed in a submerged chamber for more than 1 h in artificial cerebrospinal fluid (ACSF) that contained 138.6 mM NaCl, 3.4 mM KCl, 2.5 mM CaCl₂, 1.0 mM MgCl₂, 21.0 mM NaHCO₃, 0.6 mM NaH₂PO₄, and 10.0 mM glucose. ACSF was maintained at a pH of 7.4 by bubbling with 95% O₂–5% CO₂ gas. Unless otherwise specified, the slices were superfused with ACSF containing gabazine (5 μ M) and strychnine (2 μ M) to block both GABAergic and glycinergic⁵³ inhibitory synaptic responses. All experiments were conducted in accordance with the National Institutes of Health Guide for the Care and Use of Laboratory Animals and ARRIVE guidelines. This study was reviewed by the Institutional Animal Care and Use Committee and approved by the President of the Nippon Medical School (approval numbers: 20-021, 21-064, and 22-056).

Patch-clamp recordings

Individual slices were transferred to a recording chamber attached on the stage of a microscope (Examiner, Carl Zeiss, Japan) and continuously perfused with oxygenated ACSF at a flow rate of 1.4 ml/min and a temperature of 26–28 °C. Patch electrodes, used for whole-cell voltage-clamp recordings from DCN neurons, had resistances of 3–5 M Ω when filled with an internal solution containing (mM) potassium methanesulfonate 150.0, KCl 5.0, K-EGTA 0.1, Na-HEPES 5.0, Mg-ATP 3.0, and Na-GTP 0.4 (pH 7.4). DCN neurons were visually identified

under Nomarski optics with a water-immersion objective (40 \times , N.A. 0.80). Membrane currents were recorded with a patch-clamp amplifier (EPC-9; Heka Elektronik, Lambrecht/Pfalz, Germany). The series resistance, monitored during the experiment was less than 20 M Ω and was not compensated. Data were discarded if the series resistance changed by more than 20%. Analysis was performed using the PULSEFIT (HEKA Elektronik) and KyPlot (KyensLab Inc., Tokyo, Japan) software. All signals were filtered at 2 kHz and sampled at 10 kHz. Stimulation-evoked excitatory postsynaptic currents (eEPSCs) were recorded at a holding potential of -70 mV and evoked every 20 s by stimulation (10–30 V, 100–150 μ s) via glass microelectrodes (tip diameter 1–2 μ m) filled with ACSF and placed in the white matter surrounding the DCN. Given the stimulation site and the previous studies^{45,54,55}, the recorded eEPSCs were most likely to originate from mossy fiber inputs. eEPSCs were completely abolished by 6-cyano-7-nitroquinoxaline-2,3-dione (CNQX; 10 μ M) and DL-(-)-2-amino-5-phosphonopentanoic acid (40 μ M), confirming their mediation through ionotropic glutamatergic receptors. To monitor the paired-pulse ratio (PPR), eEPSCs were evoked with paired pulses at a 50-ms interval, and eEPSC amplitudes were measured at the peak. To construct concentration-response curves for the effects of DA and NA on eEPSC amplitude, two concentrations of agonists were sequentially administered to a single brain slice, beginning with the lower concentration, and the extent of inhibition was measured. Sequential agonist applications were performed with a sufficient time interval (more than 30 min) between successive administrations. The concentration-response curves were fitted to the following equation: $y = y_{\max} / (1 + (IC_{50}/x)^n)$, where x represents the concentration of DA or NA, n is the Hill coefficient, and y_{\max} denotes the maximum extent of depression. Free parameters were n, IC₅₀, and y_{\max} . Curve fitting was performed using KyPlot.

Chemicals

Chemicals used in this study were obtained from the following sources: NA, DA, and strychnine from Fujifilm/Wako (Osaka, Japan); clonidine, phenylephrine, (\pm)-sulpiride, and gabazine from Sigma (St. Louis, USA); and CNQX, DL-(-)-2-amino-5-phosphonopentanoic acid, dexmedetomidine, quinpirole, and RS79948 from Tocris Bioscience (Bristol, UK).

Experimental design and statistical analysis

Statistical analysis was performed using KyPlot. All data are normally distributed and expressed as mean \pm standard error of the mean (SEM), with n representing the number of independent experiments. Statistical differences were evaluated using a Student's paired *t*-test, unless otherwise noted. Both *t* values and corresponding *p* values are reported for all comparisons. Significance is reported as *p* < 0.05.

Data availability

The datasets generated during and/or analyzed during the current study are available from the corresponding author on reasonable request.

Received: 4 June 2025; Accepted: 21 August 2025

Published online: 28 August 2025

References

1. Nieoullon, A., Cheramy, A. & Glowinski, J. Release of dopamine in both caudate nuclei and both substantia nigrae in response to unilateral stimulation of cerebellar nuclei in the cat. *Brain Res.* **148**, 143–152 (1978).
2. Caragea, V. M., Méndez-Couz, M. & Manahan-Vaughan, D. Dopamine receptors of the rodent fastigial nucleus support skilled reaching for goal-directed action. *Brain Struct. Funct.* **229**, 609–637 (2024).
3. Melchitzky, D. S. & Lewis, D. A. Tyrosine hydroxylase- and dopamine transporter-immunoreactive axons in the primate cerebellum. Evidence for a lobular- and laminar-specific dopamine innervation. *Neuropsychopharmacol.* **22**, 466–472 (2000).
4. Ikai, Y., Takada, M., Shinonaga, Y. & Mizuno, N. Dopaminergic and non-dopaminergic neurons in the ventral tegmental area of the rat project, respectively, to the cerebellar cortex and deep cerebellar nuclei. *Neuroscience* **51**, 719–728 (1992).
5. Panagopoulos, N. T., Papadopoulos, G. C. & Matsokis, N. A. Dopaminergic innervation and binding in the rat cerebellum. *Neurosci. Lett.* **130**, 208–212 (1991).
6. Fujii, T., Sakai, M. & Nagatsu, I. Immunohistochemical demonstration of expression of tyrosine hydroxylase in cerebellar Purkinje cells of the human and mouse. *Neurosci. Lett.* **165**, 161–163 (1994).
7. Locke, T. M. et al. Purkinje cell-specific knockout of tyrosine hydroxylase impairs cognitive behaviors. *Front. Cell. Neurosci.* **14**, 228 (2020).
8. Flace, P. et al. The cerebellar dopaminergic system. *Front. Syst. Neurosci.* **15**, 650614 (2021).
9. Delis, F., Mitsacos, A. & Giompres, P. Pharmacological characterization and anatomical distribution of the dopamine transporter in the mouse cerebellum. *Cerebellum* **7**, 242–251 (2008).
10. Barili, P., Bronzetti, E., Ricci, A., Zaccione, D. & Amenta, F. Microanatomical localization of dopamine receptor protein immunoreactivity in the rat cerebellar cortex. *Brain Res.* **854**, 130–138 (2000).
11. Mehdizadeh, M. et al. Alteration of the dopamine receptors' expression in the cerebellum of the lysosomal acid phosphatase 2 mutant (Naked-Ataxia (NAX)) Mouse. *Int. J. Mol. Sci.* **21**, 2914 (2020).
12. Beaulieu, J. M. & Gainetdinov, R. R. The physiology, signaling, and pharmacology of dopamine Receptors. *Pharmacol. Rev.* **63**, 182–217 (2011).
13. Glaser, P. E. A. et al. Cerebellar neurotransmission in attention-deficit/hyperactivity disorder: Does dopamine neurotransmission occur in the cerebellar vermis?. *J. Neurosci. Meth.* **151**, 62–67 (2006).
14. Hong, S. & Optican, L. M. Interaction between Purkinje cells and inhibitory interneurons may create adjustable output waveforms to generate timed cerebellar output. *PLoS ONE* **3**, e2770 (2008).
15. Mittleman, G., Goldowitz, D., Heck, D. H. & Blaha, C. D. Cerebellar modulation of frontal cortex dopamine efflux in mice: Relevance to autism and schizophrenia. *Synapse* **62**, 544–550 (2008).
16. Carlson, E. S. et al. Catecholaminergic innervation of the lateral nucleus of the cerebellum modulates cognitive behaviors. *J. Neurosci.* **41**, 3512–3530 (2021).
17. Mei, Y. A. et al. Activation of dopamine D4 receptor inhibits an L-type calcium current in cerebellar granule cells. *Neuroscience* **68**, 107–116 (1995).

18. Carey, M. R. & Regehr, W. G. Noradrenergic control of associative synaptic plasticity by selective modulation of instructive signals. *Neuron* **62**, 112–122 (2009).
19. Kim, Y. S., Shin, J. H., Hall, F. S. & Linden, D. J. Dopamine signaling is required for depolarization-induced slow current in cerebellar Purkinje cells. *J. Neurosci.* **29**, 8530–8538 (2009).
20. Saitow, F., Satake, S., Yamada, J. & Konishi, S. β -Adrenergic receptor-mediated presynaptic facilitation of inhibitory GABAergic transmission at cerebellar interneuron-Purkinje cell synapses. *J. Neurophysiol.* **84**, 2016–2025 (2000).
21. Saitow, F., Suzuki, H. & Konishi, S. β -Adrenoceptor-mediated long-term up-regulation of the release machinery at rat cerebellar GABAergic synapses. *J. Physiol.* **565**, 487–502 (2005).
22. Hirono, M., Matsunaga, W., Chimura, T. & Obata, K. Developmental enhancement of $\alpha 2$ -adrenoceptor-mediated suppression of inhibitory synaptic transmission onto mouse cerebellar Purkinje cells. *Neuroscience* **156**, 143–154 (2008).
23. Di Mauro, M., Li Volsi, G. & Licata, F. Noradrenergic control of neuronal firing in cerebellar nuclei: Modulation of GABA responses. *Cerebellum* **12**, 350–361 (2013).
24. Hirono, M., Nagao, S., Yanagawa, Y. & Konishi, S. Monoaminergic modulation of GABAergic transmission onto cerebellar globular cells. *Neuropharmacol.* **118**, 79–89 (2017).
25. Lippiello, P. et al. Noradrenergic modulation of the parallel fiber-Purkinje cell synapse in mouse cerebellum. *Neuropharmacol.* **89**, 33–42 (2015).
26. Guo, A. et al. Effects of norepinephrine on spontaneous firing activity of cerebellar Purkinje cells in vivo in mice. *Neurosci. Lett.* **629**, 262–266 (2016).
27. Nelson, T. E., King, J. S. & Bishop, G. A. Distribution of tyrosine hydroxylase-immunoreactive afferents to the cerebellum differs between species. *J. Comp. Neurol.* **379**, 443–454 (1997).
28. Hökfelt, T. & Fuxe, K. Cerebellar monoamine nerve terminals, a new type of afferent fibers to the cortex cerebelli. *Exp. Brain Res.* **9**, 63–72 (1969).
29. Nedelescu, H., Chowdhury, T. G., Wable, G. S., Arbuthnott, G. & Aoki, C. Cerebellar sub-divisions differ in exercise-induced plasticity of noradrenergic axons and in their association with resilience to activity-based anorexia. *Brain Struct. Funct.* **222**, 317–339 (2017).
30. Proville, R. D. et al. Cerebellum involvement in cortical sensorimotor circuits for the control of voluntary movements. *Nat. Neurosci.* **17**, 1233–1239 (2014).
31. Carta, I., Chen, C. H., Schott, A. L., Dorizan, S. & Khodakhah, K. Cerebellar modulation of the reward circuitry and social behavior. *Science* **363**, eaav0581 (2019).
32. Washburn, S. et al. The cerebellum directly modulates the substantia nigra dopaminergic activity. *Nat. Neurosci.* **27**, 497–513 (2024).
33. Cutando, L. et al. Cerebellar dopamine D2 receptors regulate social behaviors. *Nat. Neurosci.* **25**, 900–911 (2022).
34. Faber, D. S. & Korn, H. Applicability of the coefficient of variation method for analyzing synaptic plasticity. *Biophys. J.* **60**, 1288–1294 (1991).
35. Clark, R. D. et al. (8a.alpha., 12a.alpha., 13a.alpha.)-5,8,8a,9,10,11,12,12a,13,13a,-Decahydro-3-methoxy-12-(methylsulfonyl)-6H-isoquinol[2,1-g][1,6]naphthyridine, a potent and highly selective $\alpha 2$ -adrenoceptor antagonist. *J. Med. Chem.* **32**, 2034–2036 (1989).
36. Wood, A. N. New roles for dopamine in motor skill acquisition: Lessons from primates, rodents, and songbirds. *J. Neurophysiol.* **125**, 2361–2374 (2021).
37. Aguayo, L. G. & Grossie, J. Dopamine inhibits a sustained calcium current through activation of alpha adrenergic receptors and a GTP-binding protein in adult rat sympathetic neurons. *J. Pharmacol. Exp. Ther.* **269**, 503–508 (1994).
38. Zhang, W., Klimek, V., Farley, J. T., Zhu, M. Y. & Ordway, G. A. $\alpha 2C$ Adrenoceptors inhibit adenylyl cyclase in mouse striatum: Potential activation by dopamine. *J. Pharmacol. Exp. Ther.* **289**, 1286–1292 (1999).
39. Cornil, C. A., Balthazard, J., Motte, P., Massotte, L. & Seutin, V. Dopamine activates noradrenergic receptors in the preoptic area. *J. Neurosci.* **22**, 9320–9330 (2002).
40. Cornil, C. A. & Ball, G. F. Interplay among catecholamine systems: Dopamine binds to $\alpha 2$ -adrenergic receptors in birds and mammals. *J. Comp. Neurol.* **511**, 610–627 (2008).
41. Cummings, D. F., Erickson, S. S., Goetz, A. & Schetz, J. A. Transmembrane segment five serines of the D4 dopamine receptor uniquely influence the interactions of dopamine, norepinephrine, and Ro10-4548. *J. Pharmacol. Exp. Ther.* **333**, 682–695 (2010).
42. Root, D. H. et al. Norepinephrine activates dopamine D4 receptors in the rat lateral habenula. *J. Neurosci.* **35**, 3460–3469 (2015).
43. Sánchez-Soto, M. et al. Evidence for noncanonical neurotransmitter activation: Norepinephrine as a dopamine D_2 -like receptor agonist. *Mol. Pharmacol.* **89**, 457–466 (2016).
44. Michaelides, M. et al. Dopamine D4 receptors modulate brain metabolic activity in the prefrontal cortex and cerebellum at rest and in response to methylphenidate. *Eur. J. Neurosci.* **32**, 668–676 (2010).
45. Murano, M., Saitow, F. & Suzuki, H. Modulatory effects of serotonin on glutamatergic synaptic transmission and long-term depression in the deep cerebellar nuclei. *Neuroscience* **172**, 118–128 (2011).
46. Paola, D. & Giovanna, F. On the origin of cortical dopamine: Is it a co-transmitter in noradrenergic neurons?. *Curr. Neuropharmacol.* **4**, 115–125 (2006).
47. Kempadoo, K. A., Mosharov, E. V., Choi, S. J., Sulzer, D. & Kandel, E. R. Dopamine release from the locus coeruleus to the dorsal hippocampus promotes spatial learning and memory. *Proc. Natl. Acad. Sci.* **113**, 14835–14840 (2016).
48. Beas, B. S. et al. The locus coeruleus drives disinhibition in the midline thalamus via a dopaminergic mechanism. *Nat. Neurosci.* **21**, 963–973 (2018).
49. Frau, R. et al. The potent $\alpha 2$ -adrenoceptor antagonist RS 79948 also inhibits dopamine D2-receptors: Comparison with atipamezole and raclopride. *Neuropharmacol.* **217**, 109192 (2022).
50. Alberto, C. O., Trask, R. B. & Hirasawa, M. Dopamine acts as a partial agonist for α_{2A} adrenoceptor in melanin-concentrating hormone neurons. *J. Neurosci.* **31**, 10671 (2011).
51. Saitow, F., Murano, M. & Suzuki, H. Modulatory effects of serotonin on GABAergic synaptic transmission and membrane properties in the deep cerebellar nuclei. *J. Neurophysiol.* **101**, 1361–1374 (2009).
52. Saitow, F., Nagano, M. & Suzuki, H. Developmental changes in serotonergic modulation of GABAergic synaptic transmission and postsynaptic GABA_A receptor composition in the cerebellar nuclei. *Cerebellum* **17**, 346–358 (2018).
53. Kawa, K. Glycine receptors and glycinergic synaptic transmission in the deep cerebellar nuclei of the rat: A patch-clamp study. *J. Neurophysiol.* **90**, 3490–3500 (2003).
54. Pugh, J. R. & Raman, I. M. Potentiation of mossy fiber EPSCs in the cerebellar nuclei by NMDA receptor activation followed by postinhibitory rebound current. *Neuron* **51**, 113–123 (2006).
55. Pugh, J. R. & Raman, I. M. Mechanisms of potentiation of mossy fiber EPSCs in the cerebellar nuclei by coincident synaptic excitation and inhibition. *J. Neurosci.* **28**, 10549–10560 (2008).

Acknowledgements

We thank Yasunori Mikahara of the Department of Pharmacology at Nippon Medical School for help with animal care. We would like to thank Editage (www.editage.jp) for English language editing.

Author contributions

F.S., R.A., and H.S. designed the research. F.S. performed the electrophysiological experiments. F.S., R.A., and H.S. wrote the manuscript.

Funding

This work was supported by a Grant-in-Aid for Scientific Research (grant number, 21500375) from the Ministry of Education, Culture, Sports, Science, and Technology (MEXT) in Japan (F.S.).

Declarations

Competing interests

The authors declare no competing interests.

Additional information

Correspondence and requests for materials should be addressed to F.S.

Reprints and permissions information is available at www.nature.com/reprints.

Publisher's note Springer Nature remains neutral with regard to jurisdictional claims in published maps and institutional affiliations.

Open Access This article is licensed under a Creative Commons Attribution-NonCommercial-NoDerivatives 4.0 International License, which permits any non-commercial use, sharing, distribution and reproduction in any medium or format, as long as you give appropriate credit to the original author(s) and the source, provide a link to the Creative Commons licence, and indicate if you modified the licensed material. You do not have permission under this licence to share adapted material derived from this article or parts of it. The images or other third party material in this article are included in the article's Creative Commons licence, unless indicated otherwise in a credit line to the material. If material is not included in the article's Creative Commons licence and your intended use is not permitted by statutory regulation or exceeds the permitted use, you will need to obtain permission directly from the copyright holder. To view a copy of this licence, visit <http://creativecommons.org/licenses/by-nc-nd/4.0/>.

© The Author(s) 2025